Range distribution function for energetic ions in matter

N. E. B. Cowern
Nuclear Physics Division, Atomic Energy Research Establishment, Harwell, Didcot, Oxon, OX11 ORA, United Kingdom
(Received 30 December 1981)

A method of calculating the longitudinal range distribution function for ions incident at energies much greater than that of the stopping-power maximum is presented. The effects of electronic straggling and nuclear straggling and scattering are included. Straightforward analytical results are obtained from which the longitudinal distribution is determined by simple root finding. Results are given for the illustrative cases of ^{1}H in ^{28}Si, ^{12}C in ^{12}C, and ^{27}Al in ^{9}Be. The full width at half maximum of the distribution is found to result almost entirely from electronic straggling in all cases. At high ion energies ion-nucleus collisions affect the range distribution by producing a long, low-intensity tail on the distribution, stretching towards the target surface. The shape of this tail depends principally on the relative masses of ion and target nuclei. Comparison with limited available data on proton range distributions provides support for these calculations.

I. INTRODUCTION

The calculation of longitudinal ion range distributions has been performed in the past in essentially two ways. The first method involves solving the ion transport equation indirectly to obtain moments of the range distribution.[1–11] This method does not give the exact shape of the range distribution, since there exists an infinite family of distributions which will satisfy a finite number of moment values. Nevertheless for ion energies below that of the stopping-power maximum, comparison with experimental data suggests that Pearson IV distribution functions based on the first four moments of the range distribution will give a satisfactory description.[12] Pearson III distribution functions may also give reasonable results in this region.[13] However, at energies above the stopping-power maximum, the shape of the longitudinal range distribution becomes increasingly skewed as a function of energy, and the higher moments of the distribution diverge rapidly. It is then unclear whether a moments approach is useful, although in principle a large number of moments could be used to provide additional information.[11] The second method of calculating the longitudinal range distribution involves the simulation of the ion trajectory by Monte Carlo methods,[14–17] which yields detailed sample distributions for the particular examples studied. Calculations of range distributions for energetic ions using this method,[18] together with experimental measurements,[18,19] confirm the increase in skewness towards high incident energy.

The observed skewing at high incident energy results from the increasingly small-number statistics of ion-nucleus collisions[20] in the high-energy part of the ion's trajectory, and leads to the effect recently pointed out,[21–23,17] that at high energy the full width at half maximum (FWHM) of the longitudinal range distribution is determined solely by electronic straggling. References 21 and 22 also indicated the existence of a conceptually simple analytical method for directly calculating the shape of the longitudinal range distribution function at high energy, and the first results were presented, showing the characteristic nearly Gaussian peak, and a long low-intensity tail arising from ion-nucleus scattering and energy loss. Reference 22 gave approximate formulas determining the distribution shape in the absence of electronic straggling.

The present paper derives a more precise result for the general longitudinal range distribution for ions with incident energies well above the stopping-power maximum, and includes in approximate form the effects of electronic straggling. Unlike Ref. 22, this result is applicable to all ratios of ion mass to target mass, and is limited only by the assumptions[22] that (i) the incident energy is nonrelativistic and (ii) the ions are fully stripped of their electrons throughout most of their trajectory. These assumptions are not fundamental, however, and the qualitative aspects of the result hold for all high-energy ions.

II. PHYSICAL MODEL

Several simplifications suggest themselves when one deals with the ion transport process at incident energies well above the energy of the stopping-power maximum. Firstly, the fall in stopping power towards higher energies leads to a range distribution which is determined essentially by collisions occurring at energies above the stopping power maximum. For example, protons incident on Si at 0.8 MeV (ten times the energy of the stopping-power maximum) derive about 94% of their mean range and about 85% of their standard deviation in range from collisions occurring before the ions slow down to the stopping-power maximum. These estimates are based on the range distribution tables of Littmark and Ziegler,[24] taking additional account of the probable influence of electronic straggling.[25] Towards higher energies these percentage values rapidly approach 100%. Consequently, collisions occurring at low energy (below the stopping-power maximum) may be neglected in a first approximation.

The physics of ion-nucleus collision in the high-energy region is simplified by the absence of significant screening. Following tradition[1–17,20–25] we neglect here one potential complication, namely the influence of nuclear forces on the scattering cross section. Electronic stopping is given to a good approximation by the simple Bethe theory without shell corrections, and electronic straggling is given to a first approximation by the Bohr formula.[26]

The final and most important simplification lies in the statistical treatment of ion transport. We begin by neglecting the straggling due to electronic collisions: this can conveniently be included at a later stage in the discussion. The detailed range distribution arising from ion-nucleus collisions has now to be calculated. Instead of following the usual approach by attempting to solve the Boltzmann transport equation, we note that the range distribution is in fact predominantly a single-collision distribution. This is so because the probability of an ion suffering a significant nuclear collision as it slows down from its incident energy to the energy of the stopping-power maximum is very small. Significant collisions in this context are those which contribute noticeably to the variance or higher central moments of the range distribution. The proof that this probability is small is given in the appendix to Ref. 21.

The procedure for determining the detailed range distribution is therefore to evaluate the single-collision distribution due to nuclear collisions and then to include Gaussian electronic straggling by convolving it with the nuclear distribution. The validity of the procedure follows from the independence of the electronic and nuclear collision processes.[1,25,27]

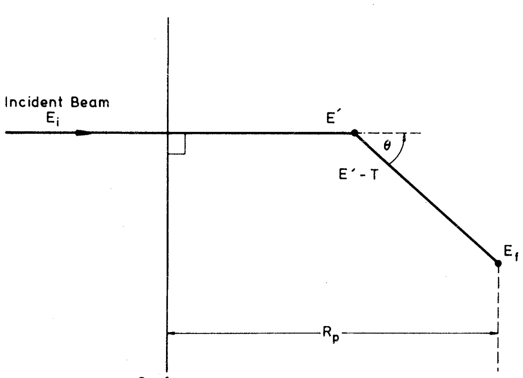

FIG. 1. Geometry of the single-scatter process leading to the longitudinal range distribution $F_n(R_p)$ of ions having final energy E_f.

III. THEORETICAL ANALYSIS

A. Calculation of $F_n(R_p)$

The geometry of the single-scatter process is shown in Fig. 1. The ion enters the target at energy E_i, and slows down at a rate given by the electronic stopping cross section S. In so doing there is a small probability that the ion will experience a significant collision at some energy E' with some energy loss T and scattering angle θ, subsequently reaching some final energy E_f at depth R_p. If $E_f \ll E_i$ then R_p is the projected range of the stopped ion. The objective is to determine the probability distribution $F_n(R_p)$, the projected range distribution due to ion-nucleus collisions.

Defining N as the number of target atoms per unit volume, and putting

$$I(E)=\int [NS(E)]^{-1}dE+\text{const} \qquad (1a)$$

one has from Fig. 1 that

$$R_p(E)=I(E_i)-I(E') +\cos\theta[I(E'-T)-I(E_f)] . \qquad (1b)$$

In the absence of a collision, one has the most probable depth

$$\hat{R}_p(E_i)=I(E_i)-I(E_f) . \qquad (1c)$$

It is convenient to define the quantity

$$\Delta R_p=\hat{R}_p-R_p \qquad (2a)$$

$$=I(E')-\cos\theta[I(E'-T)-I(E_f)]-I(E_f) . \qquad (2b)$$

The probability distribution $F_n(R_p)$ may be shown without difficulty to be

$$F_n(R_p)=\left[1-\int_{-\infty}^{\infty} y\,dR_p\right]\delta(\Delta R_p)+y \tag{3a}$$

$$y=-\int_{E_{\min}}^{E_i}\frac{1}{S}\frac{d\sigma}{dT}\left[\left.\frac{\partial R_p}{\partial T}\right|_{E'}\right]^{-1}dE' ,$$

$$(R_p)_{\min}\le R_p\le \hat{R}_p \tag{3b}$$

$$y=0,\quad R_p<(R_p)_{\min},\quad R_p>\hat{R}_p$$

provided that single-collision conditions prevail. Here $d\sigma$ is the differential cross section for energy loss $T, E_{\min}$ is the minimum value of E' for which a collision can lead to the range R_p, and $(R_p)_{\min}$ is the minimum range (corresponding to the maximum kinematically allowed energy transfer at $E'=E_i$). The first term of Eq. (3a) describes particles which have not undergone a collision, and hence arrive at depth $\hat{R}_p$, while the second term describes the single-collision depth distribution. Equations (3a) and (3b) are valid provided that

$$\int_{-\infty}^{\infty} y\,dR_p \ll 1 . \tag{3c}$$

Equations (3a) and (3b) are equivalent to the previously published expression of Vukanić and Sigmund.[28]

In the physical model to be described here, the inequality (3c) is not satisfied owing to a divergence in y as R_p approaches $\hat{R}_p$. In order to retain the attractive simplicity of the single-collision approach, I shall therefore proceed to calculate the distribution $F_n'(R_p)$, closely related to $F_n(R_p)$ and given by

$$F_n'(R_p)=(1-\epsilon)\delta(\Delta R_p)+y' , \tag{3a'}$$

$$y'=y,\quad \Delta R_p\ge\rho$$
$$y'=0,\quad \Delta R_p<\rho \tag{3b'}$$

where ρ is chosen such that

$$\epsilon=\int_{-\infty}^{\infty} y'dR_p \ll 1 . \tag{3c'}$$

It will be shown later in this paper that the use of $F_n'(R_p)$ in place of $F_n(R_p)$ has a negligible effect on the range distribution for high-energy ions, once the contribution of electronic collisions to the range straggling is included.

To evaluate $y'(R_p)$ we make assumptions about the stopping cross section S and the differential scattering cross section $d\sigma$, as remarked in Sec. II. The Bethe stopping-power formula is assumed, without shell corrections or relativistic terms, and the Rutherford elastic scattering cross section is used. Thus, defining Z_1, M_1 and Z_2, M_2 as, respectively, the atomic numbers and masses of the ion and target atoms, m_e as the mass of the electron and I_e as the mean ionization energy of the target atoms, one has

$$S=a\ln(cE)/E , \tag{4a}$$

$$a=2\pi e^4 Z_1^2 Z_2 M_1/m_e , \tag{4b}$$

$$c=4m_e/(M_1 I_e) , \tag{4c}$$

and

$$\frac{d\sigma}{dT}=k/(E'T^2) , \tag{5a}$$

$$k=\pi e^4 Z_1^2 Z_2^2 M_1/M_2 . \tag{5b}$$

To enable an analytical solution for $y'(R_p)$, Eq. (2) is expanded in powers of $\tau=T/E'$. Only a few terms are required since, for most collisions of interest, $T\ll E'$. Using the standard relation between τ and θ for elastic scattering, and applying Taylor's theorem in Eq. (2), one obtains from Eqs. (1), (2), and (4)

$$\Delta R_p=[A\tau+B\tau^2+C\tau^3+O(\tau^4)]/(Nc^2a) , \tag{6a}$$

$$A(x)=2\kappa g_0+g_1 , \tag{6b}$$

$$B(x)=(\kappa-\tfrac{1}{8})g_0-2\kappa g_1-\tfrac{1}{2}g_2 , \tag{6c}$$

$$C(x)=\tfrac{1}{8}(6\kappa-1)g_0-(\kappa-\tfrac{1}{8})g_1+\kappa g_2+\tfrac{1}{6}g_3 , \tag{6d}$$

$$g_0=\mathrm{li}(x^2)=\frac{x^2}{2\ln x}[1+\alpha(x)] , \tag{6e}$$

$$g_1=\frac{x^2}{\ln x} , \tag{6f}$$

$$g_2=\frac{x^2}{\ln x}\left[1-\frac{1}{\ln x}\right] , \tag{6g}$$

$$g_3=\frac{x^2}{(\ln x)^2}\left[1-\frac{1}{\ln x}\right] , \tag{6h}$$

where $x=cE'$, $\kappa=M_2/(4M_1)$, $\mathrm{li}(u)$ is the logarithmic integral function,[28] and $0<\alpha<0.5$ for $x\gtrsim 5$ and $\alpha\to 0$ as $x\to\infty$. $\mathrm{li}(u)$ is a special case of the confluent hypergeometric function[29] $U(m,n,z)$ with $m=n=1$ and $z=-\ln u$. It may be accurately approximated by a finite series[29] when $x\gtrsim 5$. Equation (6e) is obtained on the assumption that $\mathrm{li}(c^2E_f^2)=0$, which corresponds approximately to $E_f=1.2/c$. Since E_f may be chosen arbitrarily provided $E_f\ll E_i$, this particular value of E_f is selected on the grounds of convenience (a) that any other value leads to an additional constant in Eq. (6e), and (b) because this value is comparable with the energy of the stopping-power maximum.

In Eqs. (6) above, all terms containing the constant κ may be interpreted physically as arising from angular scattering, while the other terms arise from the energy loss in the elastic collision. The distribution function $y'(R_p)$ is given from Eqs. (3)–(5) by

$$y'(R_p)=\frac{k}{a}\int_{x_i}^{x_{\min}}\frac{1}{x\ln x}\left[-\tau^2\frac{\partial R_p}{\partial t}\bigg|_{E'}\right]^{-1}dx,$$

$$R_p \geq (R_p)_{\min},\quad \Delta R_p \geq \rho \qquad (7)$$

where $x_i=cE_i$ and $x_{\min}=cE_{\min}$. From Eq. (6a) one obtains

$$\left[-\tau^2\frac{\partial R_p}{\partial \tau}\bigg|_{E'}\right]^{-1}=\frac{A}{Nc^2a(\Delta R_p)^2}+0+\frac{Nc^2a}{A}\left[\left[\frac{B}{A}\right]^2-\frac{C}{A}\right]+\frac{O(\tau^3)}{(\Delta R_p)^2}\ . \qquad (8)$$

The convergence of the series solution for ΔR_p [Eq. (6a)] may be investigated by considering the case of slowest convergence, $\tau=\tau_{\max}$. Since the quantities $g_i(x)$ differ only slightly in their dependence on x when $x \gtrsim 5$, it is sufficient to illustrate the situation for just one value of $x=x_i$. Figure 2 shows the ratio $R_p/\hat{R}_p$ calculated for the specific case $\tau=\tau_{\max}$, $x=100$, where $\tau_{\max}$ is defined by

$$\tau_{\max}=4M_1M_2/(M_1+M_2)^2\ . \qquad (9)$$

The exact absolute value of $R_p/\hat{R}_p$ is simply given by

$$\hat{R}_p[E_i(1-\tau_{\max})]/\hat{R}_p(E_i)\ ,$$

and its sign is given by sign (M_1-M_2). The first-, second-, and third-order approximations for $R_p/\hat{R}_p$ are obtained from Eqs. (1) and (6). It is clear from Fig. 2 that convergence is rapid even when $M_1=M_2$ (i.e., when $\tau_{\max}=1$). The first-order approximation is only acceptable when $M_1 \gtrsim 10M_2$ or $M_1 \lesssim \frac{1}{30}M_2$, but the third-order approximation is quite satisfactory for all values of M_1/M_2. For values of $\tau<\tau_{\max}$ the precision in estimating R_p is even better. By differentiating the series solution for R_p with respect to τ we observe from Eq. (7) that the accuracy of the solution for $y'(R_p)$ will also be satisfactory.

Equation (8) includes a zeroth-order term (the leading term), a first-order term which is identically zero, and a second-order term which corresponds to the third-order term in ΔR_p [Eq. (6)]. In evaluating the zeroth-order term resulting from the integration in Eq. (7), the function $\mathrm{li}(x^2)$ in $A(x)$ is expressed in its infinite series form and is truncated at a suitable point, and terms containing $\ln\ln x$ are neglected. This procedure yields reliable results for $x \gtrsim 5$. In evaluating the second-order term the approximation $g_0=g_1/2$ is made; an acceptable step since for reasonably large values of x, $\alpha \ll 1$. An analytical solution can then be obtained. The solution for $y'(R_p)$ is given by

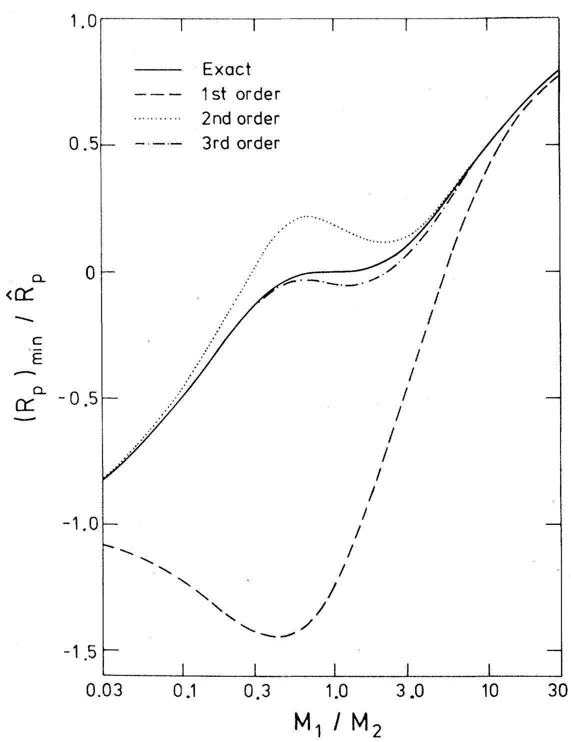

FIG. 2. Ratio of the minimum range $(R_p)_{\min}$ to the most-probable range $\hat{R}_p$, plotted as a function of M_1/M_2. The range $\hat{R}_p$ would be attained if no significant ion-nucleus collision occurred, and the range $(R_p)_{\min}$ is reached by a head-on elastic ion-nucleus collision. For the purpose of this figure, the stopping medium is assumed to extend to negative depths, so that backscattered light ions can be considered. Solid line gives the exact value of $(R_p)_{\min}/\hat{R}_p$, which has reflection symmetry about the coordinate (1.0,0) in the diagram. Other lines show, as indicated, the successive approximations obtained by following the expansion in T/E'.

$$y'(R_p)=kN^{-1}(ca\Delta R_p)^{-2}[h(x_i)-h(x_{\min})],\quad R_p\geq(R_p)_{\min},\quad \Delta R_p\geq\rho \tag{10}$$

$$h(x)=2\sum_{j=1}^{\infty}\left[(1+\kappa/j)\frac{(2\ln x)^j}{jj!}\right]-\frac{x^2}{\ln_x}$$
$$+\frac{(Nc^2a\Delta R_p)^2}{(1+\kappa)x^2}\left[-C_1-\frac{C_3}{\ln x}+(C_2-2C_3)\sum_{j=1}^{n}(-1)^j\frac{(j-1)!}{(2\ln x)^j}+R_n\right], \tag{11a}$$

$$C_1=[\tfrac{1}{16}(1+24\kappa)+\tfrac{1}{2}]^2/(1+\kappa)^2-\tfrac{1}{16}(1+6\kappa)/(1+\kappa)\,, \tag{11b}$$

$$C_2=-1/(1+\kappa)^2-(\tfrac{1}{6}-\kappa)/(1+\kappa)\,, \tag{11c}$$

$$C_3=1/[2(1+k)]^2+1/[6(1+k)]\,, \tag{11d}$$

where n is the largest integer less than $2\ln x$.

The small convergence term R_n may be neglected for $x\gtrsim 5$. $x_{\min}$ is obtained from the relation [special case of Eq. (6a)]

$$\Delta R_p=[A(x_{\min})\tau_{\max}+B(x_{\min})\tau_{\max}^2+C(x_{\min})\tau_{\max}^3]/(Nc^2a)\,. \tag{12}$$

A convenient way to obtain $x_{\min}$ from Eq. (12) is to use a zero-finding method such as bisection. For small values of $x_{\min}$ where the calculation of $h(x_{\min})$ is inaccurate, it is convenient to set $h(x_{\min})=0$ since it is in any case $\ll h(x_i)$. The criterion used here is $h(x_{\min})=0$ when

$$\Delta R_p<5\tau_{\max}/(Nc^2a)\,. \tag{13}$$

Having determined $y'(R_p)$ it is now possible to find the value of ρ [Eq. (3b′)] which is needed to satisfy the inequality $\epsilon\ll 1$ [see Eq. (3c′)]. It may be shown that

$$\epsilon=\frac{kh(x_i)}{Nc^2a^2\rho}\,. \tag{14}$$

For all ions at energies well above the stopping-power maximum, the standard deviation of the Gaussian range straggling due to electronic collisions, σ_e, is such that one can choose $\rho<\sigma_e$ while at the same time $\epsilon\ll 1$. Thus the width of the multiple nuclear-scatter distribution, which is clearly much less than ρ, must be much less than that of the electronic straggling distribution, and may be neglected when electronic straggling is included in the range distribution. Our use of $F_n'(R_p)$ in place of $F_n(R_p)$ is therefore valid.

B. Inclusion of electronic straggling

The total projected range distribution $F(R_p)$ is obtained by convolving the Gaussian electronic straggling function $F_e(\Delta R_p)$ with the distribution $F_n'(R_p)$. This yields a Gaussian with centroid at $\Delta R_p=0$ plus a very-low-intensity tail given by the convolution of a Gaussian with $y'(R_p)$ (Eq. 3a′). Although the convolution with the tail function $y'(R_p)$ cannot strictly be achieved analytically, the desired result can be reproduced quite adequately by convolving $y'(R_p)$ with a rectangular distribution with standard deviation σ_e. One obtains the approximation (good when $\epsilon\ll 1$)

$$F(R_p)=\frac{1-\epsilon}{\sigma_e\sqrt{2\pi}}\exp[-\Delta R_p^2/(2\sigma_e^2)]$$
$$+\frac{k}{Nc^2a^2}[h(x_i)-h(x_{\min})]G(R_p)\,, \tag{15}$$

where

$$G(R_p)=0,\quad \Delta R_p<\rho-\sqrt{3}\sigma_e \tag{16a}$$

$$G(R_p)=\frac{1}{2\sqrt{3}\sigma_e}\left[\frac{1}{\rho}-\frac{1}{\Delta R_p+\sqrt{3}\sigma_e}\right],\quad \rho-\sqrt{3}<\Delta R_p<\rho+\sqrt{3}\sigma_e \tag{16b}$$

$$G(R_p)=\frac{1}{2\sqrt{3}\sigma_e}\times\left[\frac{1}{\Delta R_p-\sqrt{3}\sigma_e}-\frac{1}{\Delta R_p+\sqrt{3}\sigma_e}\right],\quad \rho+\sqrt{3}\sigma_e<\Delta R_p\,. \tag{16c}$$

For large ΔR_p, Eq. (16c) reduces to $G(R_p)\simeq 1/(\Delta R_p)^2$. In Eq. (15), $h(x_{\min})$ is zero for negative values of ΔR_p: this follows automatically from the inequality (13). ρ (and hence ϵ) is chosen arbitrarily, so long as it satisfies the criterion $\rho<\sigma_e$, $\epsilon\ll 1$.

It only remains to provide an estimate of the electronic straggling standard deviation σ_e. For a first estimate the electronic energy straggling at high energy may be described by the Bohr formula.[26] This gives the second moment of the electronic single-collision energy-loss spectrum as

$$\Omega_e^2 = 4\pi e^4 Z_1^2 Z_2 \ . \tag{17}$$

Owing to the high frequency of electronic collisions as the ion slows down, the electronic contribution to the range distribution closely approximates a Gaussian, and simple use of transport theory yields the result[20]

$$\sigma_e^2 = \frac{1}{N^2}\int_{E_f}^{E_i} \frac{\Omega^2}{S^3} dE \ . \tag{18}$$

Using the stopping-power formula of Eq. (4), it is easily shown that

$$\sigma_e^2 = \frac{2m_e}{M_1}\left[\frac{1}{Nc^2 a}\right]^2 \left[\frac{2x_i^4}{\ln x_i}\alpha(x_i^2) - \frac{x_i^4}{2(\ln x_i)^2}\right] , \tag{19}$$

where α is defined as in Eq. (6e) and may easily be evaluated by a finite series approximation.

The above calculation of $F(R_p)$ is available from the author in the form of a portable Fortran code.

IV. RESULTS AND DISCUSSION

The calculation described above is suitable for all ion-target combinations, subject only to the requirements that the incident ion energy be well above the stopping-power maximum ($\gtrsim$ ten times this energy), the ions be fully stripped of their electrons at the incident energy, and that the incident energy be nonrelativistic. The results presented here are chosen to illustrate the different shapes of the elastic scattering tail due to ion-nucleus collisions, and to provide limited comparison with the small amount of experimental data available on the shape of the range distribution. Figure 3 shows the calculated range distributions of 1–100-MeV protons in ^{28}Si, together with experimental data at much lower energies[19] which are included for completeness. Backscattering causes the elastic scattering tail to extend out close to the target surface, but this tail is of very low intensity. Almost all of the incident ions come to rest in a near-Gaussian peak close to the mean range. Most importantly, the width of

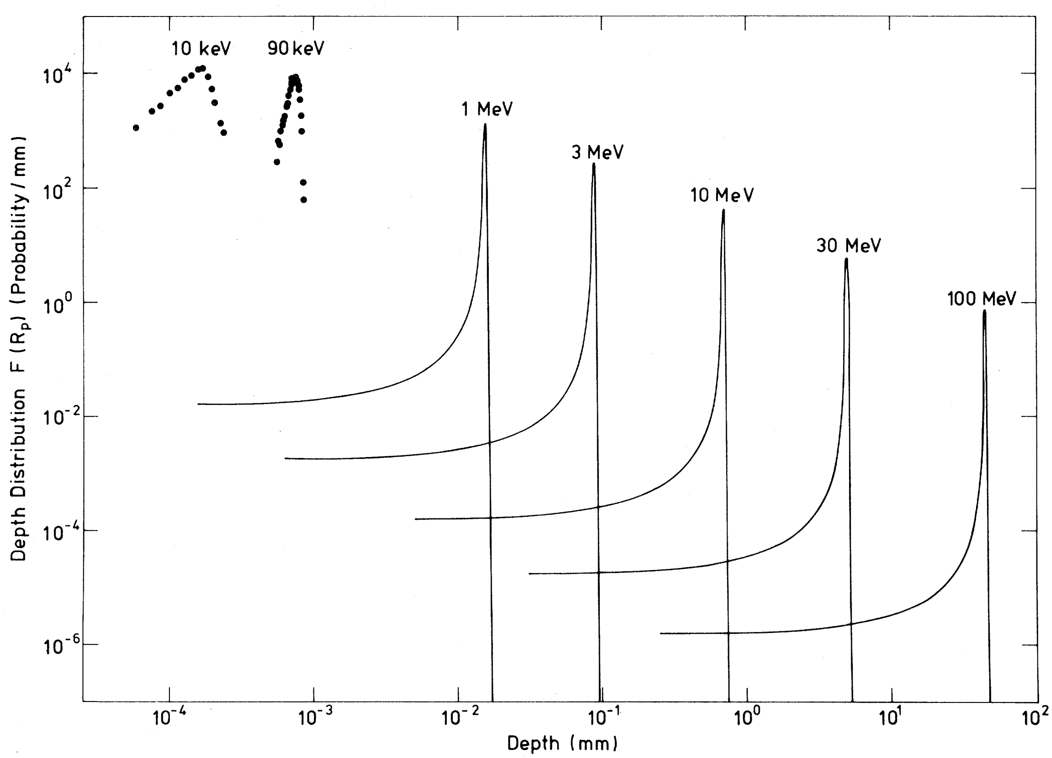

FIG. 3. Range distributions for 1–100-MeV protons in ^{28}Si, as calculated by the method described here (solid lines). Points show experimental data of Demond *et al.*[19] Experiment was not sufficiently sensitive to show the very-low-intensity tail of the distribution, but indicates the approach towards a near-Gaussian peak shape at higher energies.

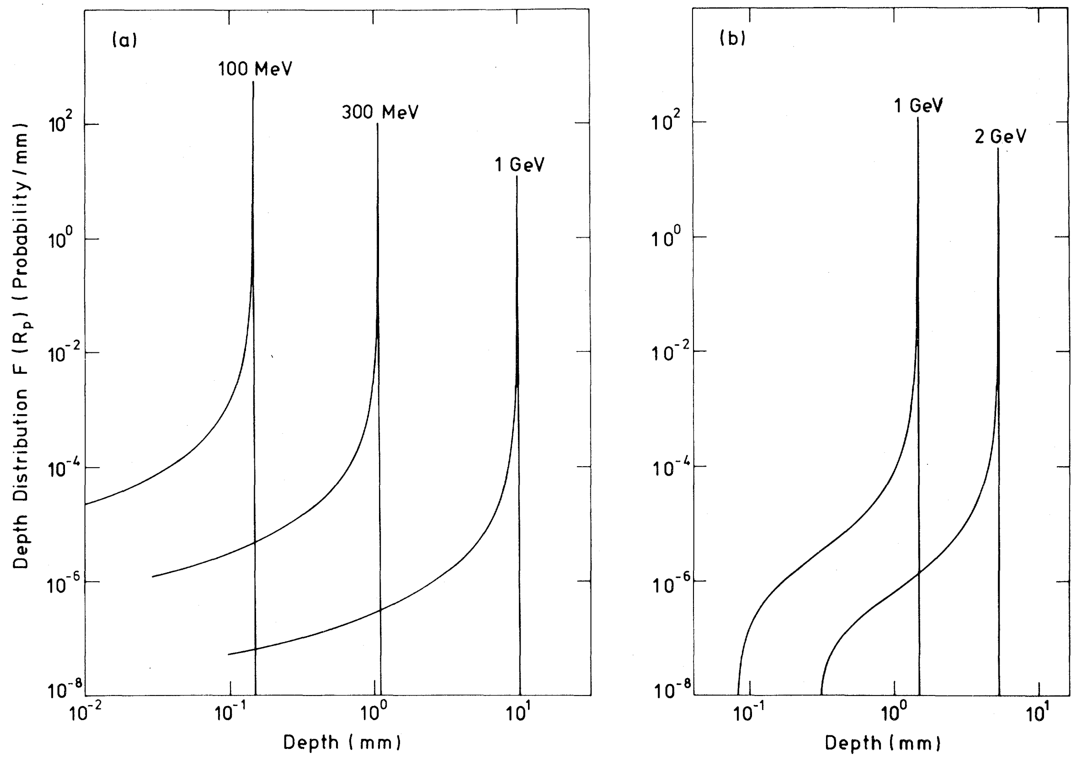

FIG. 4. Calculated range distributions for (a) 100-MeV–1-GeV ^{12}C ions in ^{12}C; and (b) 1–2-GeV ^{27}Al ions in ^{9}Be. These cases are calculated at high energy to preserve quantitative accuracy in the range. At lower energies, still well above the stopping-power maximum, the neglect of bound electrons on the ion leads to a significant underestimate in the range, but the shape of the range distribution is qualitatively the same.

this peak is determined entirely by electronic straggling. Figure 4 shows the calculated range distribution of ^{12}C ions on a ^{12}C target and ^{27}Al ions on a ^{9}Be target. In the ^{12}C-on-^{12}C case, the range distribution falls steadily towards zero as the target surface is approached, while for ^{27}Al on ^{9}Be the distribution is confined well within the target since $M_1 > M_2$. In the latter case the elastic scattering tail arises mainly from the energy loss in an ion-nucleus collision, rather than from the effect of angular scattering as may be seen from Eq. (6b) where κ is small. As in all cases, the peak shape is again nearly Gaussian, and its width is determined by electronic straggling.

It may be remarked that in previous calculations of moments of the range distribution for all ions and targets the standard deviation of the distribution was found at high energy to arise partly from elastic ion-nucleus collisions and partly from electronic straggling.[24,25] The separate contributions from these two sources were of the same order of magnitude. The way in which ion-nucleus collisions contribute to the variance is now clear: the tail of the distribution has a shape given approximately to first order by $1/\Delta R_p^2$ [Eq. (10)], while the variance weights the distribution by ΔR_p^2. Thus the extreme tail of the distribution contributes a large part of the variance, and renders this parameter worthless for experimental purposes.

If one is interested in the detailed behavior of the elastic scattering tail of the distribution, then it becomes necessary at high energy to take into account nuclear forces: a useful criterion for this is the energy at which the ion surmounts the Coulomb barrier,[30] namely,

$$E_c = \frac{Z_1 Z_2 e^2}{(A_1^{1/3} + A_2^{1/3}) r_0} ,$$

where A_1 and A_2 are the mass numbers of the ion and target nuclei, respectively, and r_0 is 1.4 fm. This may be expressed conveniently in units of MeV as

$$E_c \simeq \frac{Z_1 Z_2}{A_1^{1/3} + A_2^{1/3}} .$$

Thus, e.g., for protons at energies above a few MeV incident on Si, the tail will be substantially more intense than is calculated in Fig. 3 on the basis of Rutherford scattering. Nevertheless, the basic qualitative features of the present calculation will be unchanged, and the width of the peak of the distribution will remain essentially the same.

A comparison between the calculated Gaussian-type peak shape and experiment is possible for the case of 100-MeV protons in Al. This experiment,[31] which only measured the Gaussian-type part of the distribution, yielded a "standard deviation" of 120 ± 6 mg/cm^2. This corresponds to a FWHM of the peak of 283 ± 14 mg/cm^2. This is in fair agreement with the FWHM obtained from the present calculation for 100-MeV protons in Al of 264 mg/cm^2. Most importantly, the effect of the elastic nuclear-scattering tail on this FWHM is found to be negligible, and the deviation from a Gaussian shape is negligible down to $<\frac{1}{10}$ of the peak maximum.

A more precise treatment of electronic straggling would include electron binding effects on the energy straggling and relativistic effects in the stopping power. Such effects were included in very early work by Sternheimer,[32] which neglected nuclear collisions, and is therefore expected to provide good agreement with the experimental datum for 100-MeV protons. This is indeed the case: Sternheimer's treatment gives a standard deviation of 118 mg/cm^2 in agreement with the experiment.

V. CONCLUSIONS

An analytical treatment of the range distribution due to both electronic and nuclear collisions has been developed to describe the behavior of a wide range of ion-target combinations at incident ion energies well above the energy of the stopping-power maximum. The distribution so calculated consists of a nearly Gaussian peak whose width arises almost entirely from electronic straggling, and a long low-intensity tail which arises from elastic ion-nucleus collisions. Since many applications of range straggling are concerned with the peak width, a clear need exists for a detailed treatment of the electronic range straggling. Although Sternheimer,[32] Lewis,[33] and Janni[34] have performed such calculations for high-energy fully stripped particles, these calculations do not take into account effects arising from the presence of electrons bound to the ion. Thus for partially stripped ions the stopping power and energy straggling depend on the ionic effective charge, and the straggling is enhanced by the effects of charge exchange.[35–37] Some consideration of the charge exchange process will be required to obtain reasonable range straggling predictions for fast partially stripped ions.

[1]J. Lindhard, M. Scharff, and H. E. Schiøtt, K. Dan. Vidensk. Selsk. Mat.-Fys. Medd. 33, No. 14 (1963).

[2]H. E. Schiøtt, K. Dan. Vidensk. Selsk. Mat.-Fys. Medd. 35, No. 9 (1966).

[3]P. Sigmund and J. B. Sanders, *Proceedings International Conference* on *Application of Ion Beams to Semiconductor Technology* (Editions Orphrys, 1967), p. 215.

[4]H. E. Schiøtt, Can. J. Phys. 46, 449 (1968).

[5]J. B. Sanders, Can. J. Phys. 46, 455 (1968).

[6]K. B. Winterbon, P. Sigmund, and J. B. Sanders, K. Dan. Vidensk. Selsk. Mat.-Fys. Medd. 37, No. 14 (1970).

[7]D. K. Brice and K. B. Winterbon, *Ion Implantation Range and Energy Deposition Distributions* (IFL/Plenum, New York, 1975).

[8]K. B. Winterbon, Atomic Energy of Canada Laboratory Report No. 5536 (unpublished).

[9]U. Littmark, Institut für Plasmaphysik Report (unpublished); and U. Littmark and J. F. Ziegler, Phys. Rev. A 23, 64 (1981).

[10]J. P. Biersack, Nucl. Instrum. Methods 182/183, 199 (1981). A multiple-collision model is employed which permits use of the spherical diffusion equation rather than the usual, more general Boltzmann equation. This permits easy visualization of the ion transport process at low energy, and allows the first and second moments of the range distribution to be calculated rapidly.

[11]S. Fedder and U. Littmark, J. Appl. Phys. 52, 4259 (1981).

[12]F. Jahnel, H. Ryssel, G. Prinke, K. Hoffmann, K. Müller, J. Biersack, and R. Henkelmann, Nucl. Instrum. Methods 182/183, 223 (1981).

[13]A. F. Burenkov, F. F. Komarov, M. A. Kumakhov, and M. M. Temkin, *Tablitsy parametrov prostranstvennogo raspredeleniya ionno-implantirovannykh primeseĭ* (Izdatel'stvo BGU im. V. I. Lenina, 1980).

[14]J. E. Robinson, K. K. Kwok, and D. A. Thompson, Nucl. Instrum. Methods 132, 667 (1976).

[15]J. P. Biersack and L. G. Haggmark, Nucl. Instrum. Methods 174, 257 (1980).

[16]H. F. Kappert, K. F. Heidemann, D. Eichholz, E. te Kaat, and W. Rothemund, Appl. Phys. 21, 151 (1980).

[17]A. Luukkainen and M. Hautala, Radiat. Eff. 59, 113 (1982).

[18]D. Fink, J. P. Biersack, K. Tjan, and V. K. Cheng, Nucl. Instrum. Methods 194, 105 (1982).

[19]F.-J. Demond, S. Kalbitzer, H. Mannsperger, and G. Müller, Nucl. Instrum. Methods 168, 69 (1980).

[20]N. Bohr, K. Dan. Vidensk. Selsk. Mat.-Fys. Medd. 18, No. 8 (1948).

[21]N. E. B. Cowern, Nucl. Instrum. Methods 194, 101

(1982).
[22]N. E. B. Cowern, Phys. Rev. A 25, 604 (1982).
[23]J. P. Biersack (private communication).
[24]U. Littmark and J. F. Ziegler, *The Stopping and Ranges of Ions in Matter* (Pergamon, New York, 1980), Vol. 6.
[25]N. E. B. Cowern, Phys. Lett. 82A, 200 (1981).
[26]N. Bohr, Philos. Mag. 30, 581 (1915); N. Bohr, K. Dan. Vidensk. Selsk. Mat.-Fys. Medd. 18, No. 8 (1948).
[27]Strictly, the occurrence of a large energy-loss nuclear collision inserts a gap in the integral over energy which reduces the range straggling due to electronic collisions. Also, the scattering angle on a nuclear collision tends to reduce the projected electronic range straggling. However, in practice these effects are insignificant since electronic straggling is important near the maximum of the range distribution where the corresponding nuclear energy losses and scattering angles are small.
[28]J. Vukanić and P. Sigmund, Appl. Phys. 11, 265 (1976).
[29]M. Abramowitz and I. A. Stegun, *Handbook of Mathematical Functions* (Dover, New York, 1965).
[30]W. E. Burcham, *Nuclear Physics* (Longmans, New York, 1963).
[31]P. M. Portner and R. B. Moore, Can. J. Phys. 43, 1904 (1965).
[32]R. M. Sternheimer, Phys. Rev. 117, 485 (1960).
[33]H. W. Lewis, Phys. Rev. 85, 20 (1952).
[34]J. F. Janni, Air Force Weapons Laboratory Report No. TR-65-150 (unpublished).
[35]O. Vollmer, Nucl. Instrum. Methods 121, 373 (1974).
[36]N. E. B. Cowern, Harwell Report No. AERE-R 9500 (unpublished). .
[37]C. J. Sofield, N. E. B. Cowern, and J. M. Freeman, Nucl. Instrum. Methods 170, 221 (1980).